MINISTRY OF EDUCATION AND TRAINING

VIETNAM ACADEMY OF SCIENCE AND TECHNOLOGY

GRADUATE UNIVERSITY OF SCIENCE AND ECHNOLOGY

Ngo Nhu Viet

INVESTIGATING ELECTROMAGNETIC WAVE ABSORPTION PROPERTIES VIA RESONANT INTERACTION IN MULTILAYER METAMATERIALS

SUMMARY OF DISSERTATION ON MATERIALS SCIENCE

Major: **Electronic material**

Code: 9 44 01 23

Ha Noi - 2025

The dissertation is completed at: Graduate University of Science and Technology, Vietnam Academy Science and Technology

Supervisors:

1. Supervisor 1: Dr. Bui Son Tung, Graduate University of Science and Technology, Vietnam Academy Science and Technology
2. Supervisor 2: Prof. Dr. Vu Dinh Lam, Graduate University of Science and Technology, Vietnam Academy Science and Technology

Referee 1: Assoc. Prof. Dr. Trinh Xuan Hoang

Referee 2: Assoc. Prof. Dr. Nguyen Thanh Binh

The dissertation was defended before the Doctoral Dissertation Evaluation Council at the Graduate University of Science and Technology, Vietnam Academy of Science and Technology, at 09:00 a.m., November 28, 2025.

The dissertation can be found at:

1. Graduate University of Science and Technology Library
2. National Library of Vietnam

INTRODUCTION

1. The urgency of the dissertation

Metamaterial absorbers (MAs) are artificially engineered materials that are specifically designed to efficiently absorb electromagnetic waves within a certain frequency range [10–12]. The concept of metamaterial absorbers was first introduced in the study by Landy et al. [13], opening a new research direction in the field of metamaterials. Since then, numerous scientific studies worldwide have focused on developing and expanding the applications of MAs across different frequency regions, including the terahertz (THz) region [14] and the gigahertz (GHz) region [15]. Although single-layer MAs can be designed to achieve high absorption efficiency within a specific frequency band, they typically exhibit only a single dominant absorption peak and are limited in their ability to tune characteristics such as the position, number, and intensity of absorption peaks. In addition, the absorption properties of MAs are significantly influenced by the incident angle and polarization of the electromagnetic waves [17]. To overcome these limitations, multilayer metamaterial absorbers (MMAs) have been proposed. Multilayer structures enable optimization and extension of absorption characteristics by adjusting the thickness, stacking order, and geometric design of each layer. As a result, the absorption performance can be significantly enhanced, while the absorption region can be broadened compared to single-layer MA structures [18–19]. It can be seen that the investigation of MMAs makes it possible to achieve properties such as broadband absorption and multi-peak absorption, thereby opening up numerous application opportunities for this type of material in energy harvesting, electromagnetic shielding, sensing, and related fields. Therefore, the doctoral candidate selected the research topic: “Investigation of electromagnetic wave absorption properties based on resonant interactions in multilayer metamaterial structures”. Domestically, this dissertation topic

demonstrates distinctive features and novel contributions compared to previous studies on MAs [17], [22–25]. Although these studies investigated various types of MAs, they primarily focused on single-layer MA structures. In contrast, this dissertation concentrates on multilayer metamaterial absorbers in order to clarify the absorption mechanisms, interlayer interactions, and their resulting properties.

2. The objectives of the dissertation

Design and Analysis: To design MMA capable of multi-band and broadband absorption, and to explore the possibility of switching between EIT (Electromagnetically Induced Transparency) and EIA (Electromagnetically Induced Absorption).

Mechanism Elucidation: To clarify the mechanism of interaction between the layers within the structure.

Role of Losses: To elucidate the role of material loss components (Ohmic and dielectric losses) in the overall performance

3. Content of the Research

The thesis involved designing and simulating MMA structures using CST software, and fabricating them through photolithography. A combined methodology of calculation, simulation, and experimental measurement was employed to evaluate the electromagnetic properties (absorption, reflection, and transmission). The scope of the research focuses on the interaction between layers within the MMA in the GHz and THz frequency ranges.

4. Scientific and Practical Implications

This research has scientific merit by modeling and elucidating the operational mechanisms and interlayer interactions within MMA structures. Practically, the findings offer valuable contributions toward the application of MMA in fields such as energy harvesting, electromagnetic shielding, and sensing.

5. Novel Contributions

In this thesis, several MMA structures were successfully proposed and fabricated. These MMA structures were designed based on the principle of electromagnetic resonance at specific frequencies, where the dielectric and conductive layers play a key role in tuning the absorption bandwidth.

The interaction mechanism between the structural layers was elucidated through investigations of the absorption spectrum, surface current distribution, magnetic field, and electric field in the MMA samples. Simulation results indicate the potential for expanding MMA applications, particularly in broadband absorption, polarization tuning, and optoelectronic sensor integration.

Furthermore, the dissertation also involved the study and simulation of multifunctional MMA structures, demonstrating the ability to switch between EIT and EIA effects.

Thesis Structure

The dissertation comprises 145 pages, including an Introduction, five content chapters, and the Conclusions.

CHAPTER 1. OVERVIEW OF MULTILAYER METAMATERIAL ABSORBERS OF ELECTROMAGNETIC WAVES

1.1. Introduction to electromagnetic wave metamaterial absorbers

1.1.1. Metamaterials: a general overview

Metamaterials (MM), named from the Greek for “beyond” are synthetic composites made from materials like plastics and metals. Their electromagnetic properties arise from the geometry of engineered subwavelength structures rather than their chemical makeup. By designing periodic patterns, key parameters such as permittivity, permeability, and refractive index can be precisely controlled. Due to their remarkable characteristics, MMs are now employed across numerous applications, including superlenses [7], [29], [30], invisibility cloaks [8], [31],

[32], perfect absorbers (MPA) [9], [33], [34], and sensors [35], [36], [37].

1.1.2. Definition, classification, and evolution of metamaterial absorbers

MA is an MM variant specially engineered for effective electromagnetic energy absorption across specific frequency ranges. Its absorption performance is predominantly dictated by its artificial microstructure, rather than its constituent chemical elements.

MA can be classified according to various criteria. Specifically, they can be divided into broad-band and narrow-band, depending on their absorption bandwidth [38], [39]. Additionally, Metamaterial Absorbers can be categorized based on their operating frequency range, including MA working in the microwave, THz, and optical regions.

1.2. Mechanism of operation for metamaterial absorbers

1.2.1. Electric and magnetic resonances in metamaterials

Magnetic resonance results from the array's geometric interaction with the incident wave's magnetic component. At resonance, this interaction induces displacement or circulating currents within the structure, creating a strong effective magnetic response, which can cause the effective permeability (p) to become negative [44], [45].

Magnetic resonance occurs through the generation of induced circulating currents in loop-like elements, such as SRRs or closed/semi- closed loops, upon interaction with the incident wave's magnetic field component. At resonance, these eddy currents are highly amplified, creating a secondary induced magnetic field. This field can lead to the phenomenon of negative magnetic permeability (p), a unique property not found in natural materials [45], [46].

1.2.2. Impedance matching theory

Impedance matching aims to tune the electromagnetic characteristics of the

MA so that its impedance closely matches the wave impedance of the surrounding medium. This minimizes reflection at the surface and maximizes the transmission of energy into the absorbing layer. Once the electromagnetic wave enters the material, its energy is further dissipated through internal loss processes, which are determined by the geometric design and electromagnetic parameters of each structural component.

1.2.3. Energy dissipation mechanisms in metamaterials

Dielectric loss occurs in the non-conductive host material, where energy is dissipated when polarizing dipoles oscillate or reorient in response to the applied external electric field. As the electromagnetic wave interacts with the material, these dipoles undergo vibration and lose energy via internal molecular friction, which manifests as heat [53].

Ohmic loss primarily occurs in the thin metallic layers of the MA. When an electromagnetic wave reaches the conductive layer, it activates induced currents-currents that are forced to oscillate by the incident wave field. This process generates heat due to the metal's internal resistance within the MA structure.

1.3. Multilayer metamaterial absorbers of electromagnetic waves

1.3.1. Broadband multilayer metamaterial absorbers

The stacking of layers in MMA plays a crucial role in broadening the absorption bandwidth and enhancing the material's efficiency. Each layer in the multilayer structure typically includes distinct resonant elements, such as small metallic patterns or graphene structures placed on a dielectric substrate. When these layers are stacked, they create multi-level resonances with various resonance points, corresponding to multi-band or broadband absorption frequencies [58], [77-78].

1.3.2. Multifunctional multilayer metamaterials

Furthermore, MMA are employed to obtain enhanced absorption at multiple distinct frequencies [61]. The increased absorption capability in MMA can be achieved by switching between EIT and EIA effects [61], [84]

1.3.3. Applications of multilayer electromagnetic wave absorbing metamaterials

MA can be engineered using multilayer configurations comprising diverse materials to optimize the absorbing structure and enhance their absorption capabilities [88], [89], or to provide effective shielding against electromagnetic radiation [90]. These MMA find applications across various fields, including energy harvesting [91] and sensing [92].

1.4. Conclusion of Chapter 1

This chapter presents the fundamentals of MAs. It then analyzes and evaluates their operating mechanisms, including electric and magnetic resonance, impedance matching, and energy dissipation theory. Additionally, the chapter introduces various MMA structures with different mechanisms and discusses several key MMA applications.

CHAPTER 2. RESEARCH METHODOLOGY

2.1. Theoretical research method

2.1.1. Simulation methodology

Specialized software packages such as CST Microwave Studio, HFSS, and COMSOL are commonly used to design and simulate MM. They allow for the simulation of materials in either 2D or 3D space. The electromagnetic properties of an MM can be determined by simulating a single unit cell structure, completely defining the parameters, material types, and appropriate boundary conditions.

2.1.2. Equivalent LC circuit model

The electromagnetic properties of MA can be predicted and explained based on the equivalent RLC circuit model. The RLC circuit model depends on

the MA's structural configuration, where the metallic layers are replaced by inductors with effective inductance L and capacitors with effective capacitance C. The values of L and C are calculated based on the structural geometry and the electromagnetic energy distribution. Each metal-dielectric layer corresponds to a single RLC circuit, and consequently, an MMA structure is modeled as a series of RLC circuits [87], [93-95].

2.1.3. Coupled oscillator model

EIT is understood as a quantum interference phenomenon between different excitation sources. Initially, a first excitation source is introduced into the medium, which absorbs waves from this source as the medium is considered opaque to it. Subsequently, the medium is simultaneously subjected to a second excitation source, from which it can also absorb waves. At this point, an interference effect occurs that converts the absorption property into a transmission property, and vice versa [97-99].

2.2. Fabrication method

Photolithography is a pervasive material fabrication technique enabling the creation of precisely shaped and sized features. Its principle relies on using light radiation to change the characteristics of a photoresist layer coated on the material surface. The photoresist, a photosensitive organic compound, remains robust in alkaline or acidic media, protecting the material details from subsequent etching.

2.3. Measurement method for electromagnetic properties of multilayer metamaterials

The Vector Network Analyzer (VNA) system at the Institute of Materials Science, Vietnam Academy of Science and Technology, is used to determine the reflectance and transmittance of MA and MMA. This system features two antennas serving as the source and receiver, whose positions are adjusted based on the required measurement. The output of the measurement is the complex S-

parameters, which characterize the reflective and transmissive properties of the MA and MMA.

2.4. Conclusion of Chapter 2

The CST Microwave Studio software is used to optimally design the MA and MMA structures. Computational methods are implemented to compare, correlate, and further optimize these designs. Based on both simulation and calculation, the MMA are fabricated primarily via photolithography and other methods. Post-fabrication, the electromagnetic properties of the samples are measured using a Vector Network Analyzer (VNA) system. The resulting experimental data is then compared and correlated with the simulation and computational findings.

CHAPTER 3. INTERLAYER INTERACTION EFFECTS ON ABSORPTION PROPERTIES OF MULTILAYER METAMATERIALS IN THE GHz RANGE

3.1. Effect of metal loss on interlayer interaction and absorption performance

3.1.1. MMA with low ohmic loss

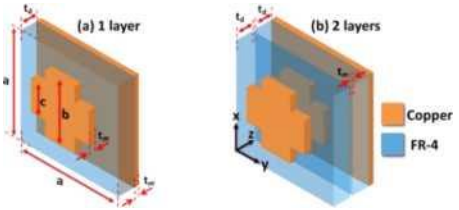

Figure 3.1. *Simulated Structure: (a) Single-Layer and (b) MMA*

A MA comprises a metal-dielectric layer situated on a continuous metallic backplate, with a unit cell size of a. The MMA is created by increasing the number of these metal-dielectric layers. In the metal-dielectric layer, the metal component is patterned with a cross-shaped structure having a thickness of t_m, a length of b,

and a width of c, and it is placed on a continuous dielectric substrate of thickness t_d. The continuous metallic backplate at the bottom has a thickness of t_b. The structural parameters of the unit cell are set as follows: a=18 mm, b=16 mm, c=7 mm, t_b=0.035 mm, and t_m=0.035 mm. The dielectric material used is FR-4, with a relative permittivity of ε=4.3 and a loss tangent of $tan\delta$=0.025. The metallic layers are made of copper with an electrical conductivity of $\sigma = 5.96 \times 10^7$ S/m.

The MMA structure yields an absorption spectrum with absorption exceeding 90% in the frequency range of 4.84-5.02 GHz, as shown in Figure 3.2(a). There are two maximum absorption peaks at 4.89 GHz and 4.97 GHz, with absorption values of 98.99% and 98.44%, respectively.

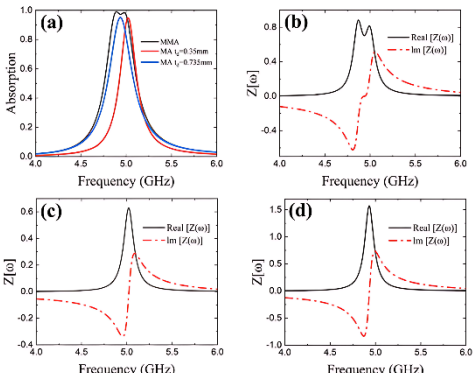

Figure 3.2. *(a) Absorption spectra of the multilayer MA and single-layer ones with two different die- lectric layer thicknesses. (b) Effective impedance of the multilayer MA, and single-layer ones with td = (c) 0.35 and (d) 0.735 mm.*

The equivalent circuit model for the MMA is illustrated in Figure 3.10(a). Figure 3.10(b) presents the calculated spectrum of the total current for the circuit model for both the single-layer MA and the MMA. In the case of the MA, a single absorption peak appears at 4.95 GHz. Conversely, for the MMA, the shape of the calculated spectrum aligns with the shape of the simulated absorption spectrum, showing two distinct peaks at 4.73 GHz and 5.01 GHz. A comparison of the experimental and simulated absorption spectra for the MA and MMA is provided

in Figures 3.10(c) and 3.10(d). For the MA structure, both simulation and experimental results show a single peak at 5.02 GHz and 5 GHz, with absorption values of 94.7% and 90.3%, respectively. For the MMA, in the simulation, the proposed multilayer structure achieves an absorption greater than 90% in the frequency range of 4.84-5.02 GHz. The experimental absorption reaches 90% over a broader frequency range of 4.72-5.18 GHz.

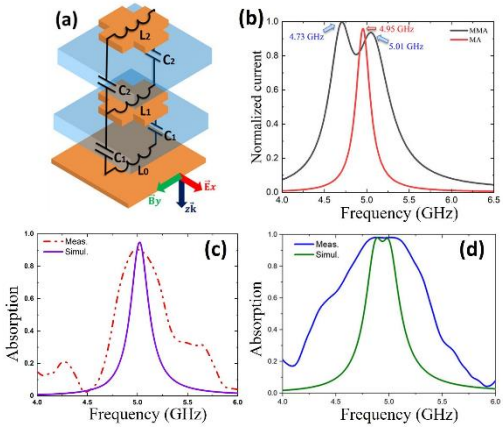

Figure 3.10. *(a) Equivalent-circuit models of the MMA. (b) Calculation of the normalized total current in the single MA and MMA, according to the LC circuit model. Measured and simulated absorption spectra of (c) the single-layer and (d) MMA*

The MMA proposed consists of two circular ring-shaped resonant layers (Figure 3.11). The proposed MMA exhibits an absorption peak at 4.31 GHz with an absorption rate of 98.9%. It is characterized by its insensitivity to the angle of incidence for both mode TE and TM polarizations. The unit cell size is $a = 20$ mm. The metallic resonant structure is designed as a circular resonant ring with a thickness of $t_m = 0.036$ mm, an outer radius of $R_1 = 8.5$ mm, and an inner radius of $R_2 = 2.5$ mm. The dielectric material used is FR-4, which has a relative permittivity of $\varepsilon = 4.3$ and $tan\delta = 0.025$ with a thickness of $t = 0.9$ mm. The metallic layers are made of copper, with an electrical conductivity of $\sigma = 5.96 \times 10^7$ S/m.

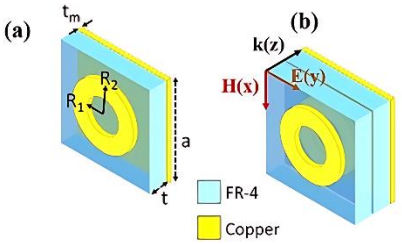

Figure 3.11. *Design Diagram of (a) MA and (b) MMA*

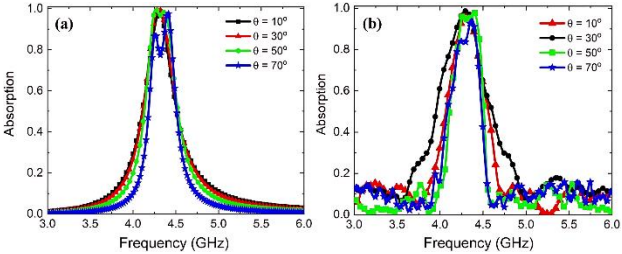

Figure 3.16. *(a) Simulated and (b) experimental absorption spectra of MMA at different incident angles under TE polarization, including 10°, 30°, 50°, and 70°*

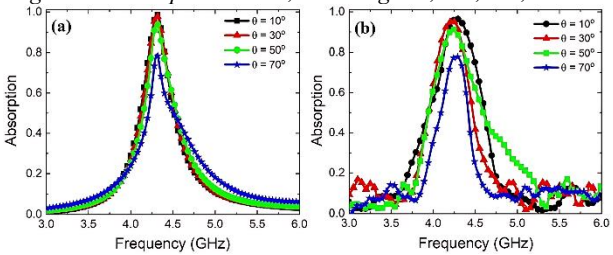

Figure 3.17. *(a) Simulated and (b) experimental absorption spectra of MMA at different incident angles under TM polarization, including 10°, 30°, 50°, and 70°*

Under normal incidence, the absorptivity increases from 93.1% for the monolayer to 98.9% for the multilayer structure. Furthermore, the MMA exhibits high angular stability, maintaining an absorption peak of approximately 97.5% even at an oblique incidence of 70°. In contrast, under TM-polarized waves, a gradual decline in absorption performance is observed as the incident angle increases.

3.1.2. MMA exhibits high ohmic losses

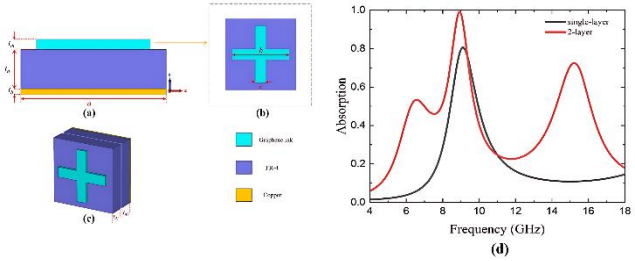

Figure 3.18. *Proposed MA and MMA structures: (a) MA, (b) Resonant layer design, (c) MMA, and (d) Absorption spectrum of MA and MMA with a Graphene absorber layer (2Ω/sq).*

The MA structure comprises a cross-shaped graphene layer with length b, width c, and thickness t_g (Figure 3.18 b), and an FR-4 dielectric layer with thickness t_d placed atop a continuous copper metallic plate of thickness t_m. The unit cell size is a. FR-4 is used with a dielectric constant $\varepsilon = 4.3$ and a loss tangent of 0.025. The electrical conductivity of copper is 5.96×10^7 S/m, while the conductive graphene ink has a varying surface resistance. Figure 3.18 c depicts the MMA structure, which consists of two graphene-FR-4 layers of the same dimensions and design as the MA, placed on a continuous copper metallic plate.

Figure 3.18 d shows that the graphene MA exhibits one absorption peak at a frequency of 9.1 GHz with a relatively low absorbance of 80.55%. When the number of layers increases to two, the number of absorption peaks rises to three within the 4-18 GHz frequency range. The MA structure exhibits an absorption spectrum with a peak at a frequency of 9.57 GHz, reaching an absorbance of 99.57%. Concurrently, the structure also achieves an absorption bandwidth of 5.22 GHz, with the absorbance exceeding 90% within the 7.37-12.59 GHz frequency range. The MMA structure features absorption peaks at 8GHz and 12.16 GHz, reaching 96.86% and 98.29%, respectively. This structure demonstrates a broad absorption bandwidth exceeding 8.43GHz, with the absorbance surpassing 90% in the 6.07-14.5GHz frequency band.

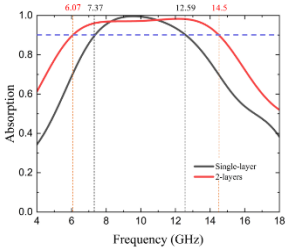

Figure 3.24. *Absorption spectra of MA (t_d=3.5mm) and MMA (t_{d1}=t_{d2}=1.7mm) with a graphene absorber layer (100Ω/sq)*

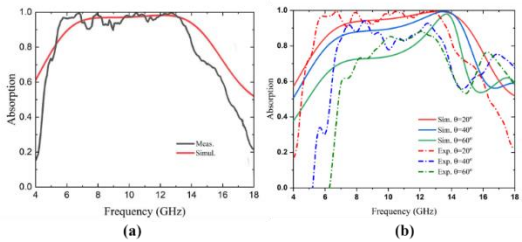

Figure 3.36. *(a) Experimental and simulated absorption spectra of graphene MMA. (b) Experimental absorption spectra of graphene MMA at various incidence angles.*

Figure 3.36a illustrates the experimental and simulated absorption spectra of the proposed MMA structure. The simulated and experimental results show excellent agreement, confirming that the fabricated MMA structure achieves an absorbance exceeding 90% in the 5.43 to 13.65GHz frequency range.

3.2. Influence of the dielectric on the interaction

As shown in Figure 3.37, observing the absorption spectra of the MMA structure reveals that the absorbance gradually decreases as the dielectric loss tangent (tanS) is reduced from 0.025 to 0.0022. At frequencies of 4.85 GHz and 4.96 GHz, the absorbance reaches 69.67% and 71.26% when tanS=0.0022. The results clearly indicate the influence of the dielectric, or more specifically, the dielectric loss, on the absorption capability of the MMA structure.

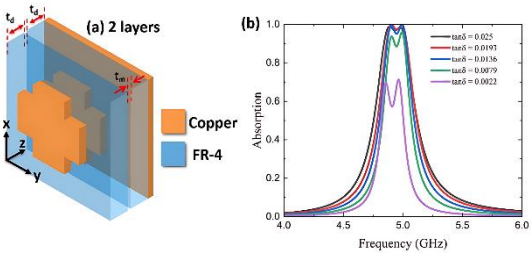

Figure 3.37. *(a) Schematic of the MMA structure, (b) Absorption spectra of MMA with varying tanô (loss tangent).*

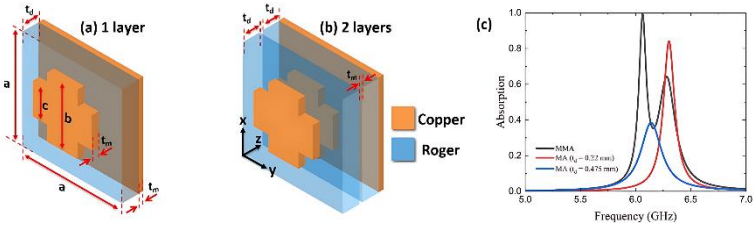

Figure 3.38. *(a) Schematic of the Single-layer MA structure, (b) MMA structure, and (c) Absorption spectra of MA and MMA.*

The structural parameters of the unit cell are set as a=18mm, b=16mm, c=7mm, t_b=0.035mm, t_d=0.035mm, and t_m=0.035mm. The absorption spectra of the MA and MMA structures are presented in Figure 3.38 c. The MA exhibits an absorption peak at a frequency of 3.13GHz with an absorbance of 89.94%. The absorption spectrum of the MMA structure shows two absorption peaks, reaching 95.1% and 69.41% at frequencies of 3.03 GHz and 3.14 GHz, respectively.

3.3. Conclusion of Chapter 3

Research indicates that in two-layer MMA structures, **low-loss materials** (Cu-FR4, Cu-Roger) produce distinct magnetic resonance peaks within narrow bands, such as 4.89–4.97 GHz or 6.06–6.28 GHz. Conversely, using **high-loss materials** (Graphene conductive ink) causes adjacent resonance peaks to merge, significantly broadening the absorption spectrum. Experimental results demonstrate that Graphene-based MMAs achieve over 90% absorption across a

wide frequency range of 6.07–14.5 GHz, reaching an FBW of 81.96%, which far outperforms low-loss structures.

CHAPTER 4. THE INFLUENCE OF INTER-LAYER INTERACTION ON THE ABSORPTION PROPERTIES OF MULTILAYER METAMATERIALS IN THE THz FREQUENCY RANGE

4.1. Influence of the metal on interlayer interaction and absorption performance

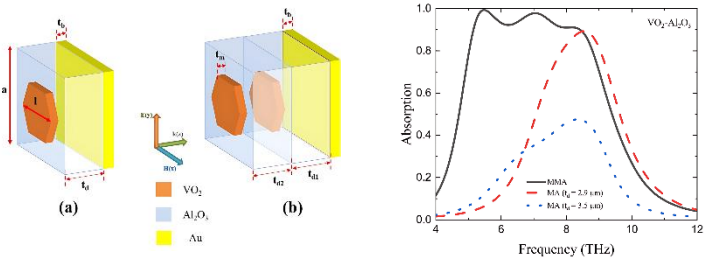

Figure 4.1. Structural diagrams of (a) monolayer MA, (b) bilayer MMA with VO_2 absorption layer, (c) absorption spectra of MMA and monolayer MA (σ = 17500 S/m).

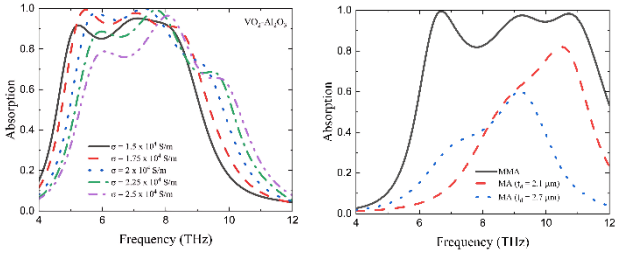

Figure 4.7. Absorption spectra of (a) MMA with different VO_2 conductivity; (b) MA and MMA with VO_2 absorption layer (σ = 25000 S/m)

When the VO_2 conductivity is 17.500 S/m (high Ohmic loss), the MMA operates as a broadband absorber covering 5.16–8.41 THz with an FBW of 47.89%. Increasing the conductivity to 25.000 S/m (low Ohmic loss) shifts the performance to a multi-resonant state, characterized by three intense absorption peaks at 6.68, 9.24, and 10.7 THz.

4.2. Influence of dielectric properties on interlayer interaction and absorption characteristics

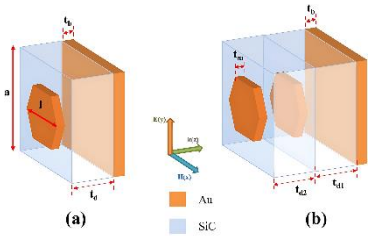

Figure 4.11. *(a) Schematic of the Au-SiC MA structure, (b) MMA.*

The Au-SiC MMA structure was proposed, as shown in Figure 4.11. The MMA exhibits two maximum absorption peaks at 22.84 THz and 23.06 THz, with corresponding absorbances of 98.77% and 95.62%. The absorption bandwidth exceeding 90% absorbance achieved an FBW value of 1.78%.

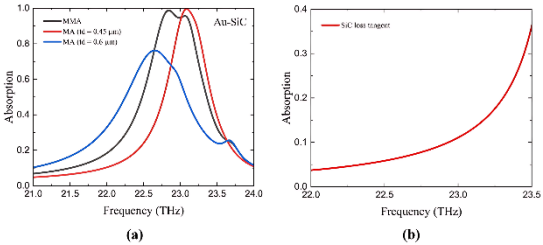

Figure 4.12. *(a) Absorption spectra of Al-SiC-based MA and MMA, and (b) dielectric loss of SiC*

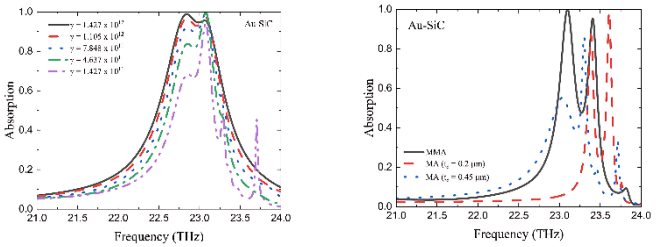

Figure 4.17. *Influence of the dielectric loss coefficient Y on the absorption properties of the MMA, and the absorption spectra of the MMA and single-layer MA with γ = 1.427 x 10^11*

The absorption spectra of the Au-SiC MA and MMA structures with γ=1.427 x 10^{11} are presented in Figure 4.17. The MMA structure exhibits two

absorption peaks at frequencies of 23.09 THz and 23.4 THz, achieving absorbance values of 99.96% and 95.21%, respectively.

4.3. Application of MMA in Infrared Emission

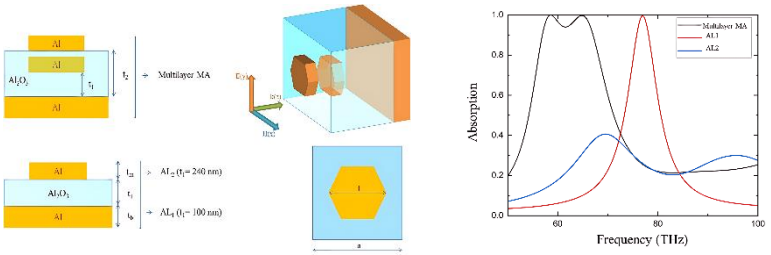

Figure 4.23. *Single-layer MA and MMA structures, and the absorption spectra of MA and MMA.*

The unit cell of the proposed MMA has a dimension of a and consists of two layers. The structural parameters of the unit cell are optimized with the following values: a = 1500 nm, t_b = 200 nm, t_1 = 100 nm, t_m = 100 nm, t_2 = 240 nm, and l = 300 nm. Figure 4.23 illustrates the absorption spectra of the proposed MMA and the single-layer hexagonal MA. The results indicate that the AL1 (t_1 = 100 nm) and AL2 (t_1 = 240 nm) structures exhibit two absorption peaks at 41.3 THz and 69.5 THz, with absorptivities of 94% and 40%, respectively. In comparison, the combined AL1 + AL2 structure yields superior simulated absorption performance, achieving an absorptivity exceeding 90% within the frequency range of 56.9 – 67.9 THz.

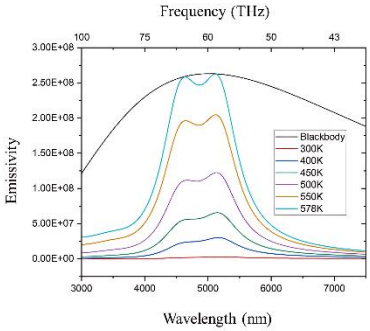

Figure 4.24. *Comparison of the emission intensity of the MA at various temperatures with the emission intensity of an ideal blackbody.*

The emission intensity of the MA structure, as illustrated in Figure 4.24, exhibits an upward trend with increasing temperature. At 300 K, the emission is nearly negligible. From 400 K onwards, the emission band broadens and the intensity gradually increases, while the peak positions remain constant. At 578 K, the emission intensities at 4632 nm and 5115 nm reach values approximately equal to those of an ideal blackbody.

4.3. Conclusion of Chapter 4

The chapter clarified inter-layer interaction by investigating MMAs with varying Ohmic losses and the influence of dielectric loss in the THz frequency range:

- High Ohmic Loss (VO_2-Al_2O_3): The MMA achieved broadband absorption (FBW=47.89%), maintaining >90% absorbance between 5.16-8.41THz (σ=17500S/m).

- Low Ohmic Loss (VO_2-Al_2O_3, σ=25000S/m): The electromagnetic properties were simulated.

- Dielectric Loss (Au-SiC): Simulation of high- and low-loss MMAs showed that the high-loss case resulted in two absorption peaks.

CHAPTER 5. RESEARCH ON MULTILAYER MULTIFUNCTIONAL METAMATERIAL STRUCTURES

5.1. Research on multilayer multifunctional metamaterial structures operating in the ghz frequency range

The multi-functional MMA structure is designed with three different single-layer MA structures, as shown in Figure 5.1. The structural parameters are presented in Table 5.1.

When the distance between the layers was optimized, the MMA achieved a maximum absorption spectrum value of 94.36% at a frequency of 4.36 GHz, and subsequently, the absorption decreased when $d_1=3$ mm.

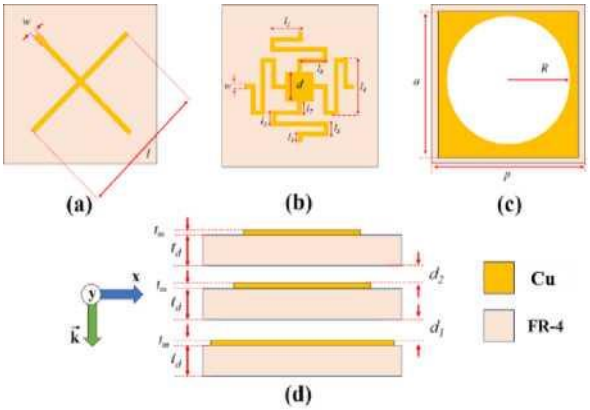

Figure 5.1. *Schematic diagram of the design of a multi-functional MMA structure operating in the GHz frequency range, showing (a) the top layer, (b) the middle layer, (c) the bottom layer, and (d) the overall structure.*

Parameters	*p*	t_d	t_m	*a*	*R*
Value (mm)	15	0.4	0.035	13.5	6
Parameters	*d*	*l1*	*l2*	*l3*	*l4*
Value (mm)	2.5	1.5	3	1.5	7
Parameters	l_5	*l6*	l_7	*w*	*l*
Value (mm)	1.5	3	1	0.5	12

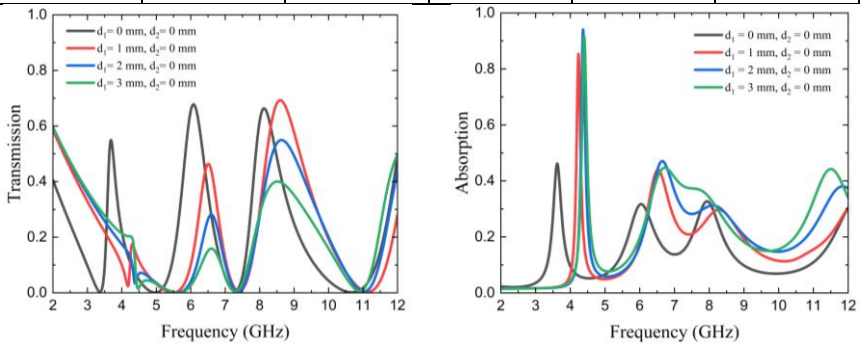

Figure 5.3. *(a) Transmission spectra and (b) absorption spectra of the MMA structures.*

5.2. Research on multi-layer multi-functional metamaterial structure operating in the THz frequency range

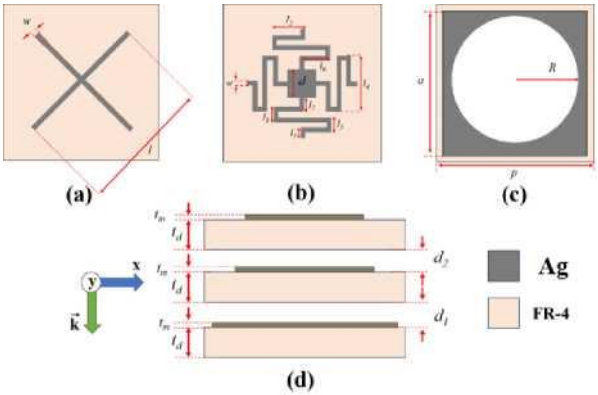

Figure 5.6. *Schematic diagram of the design of a multi-functional MMA structure operating in the THz frequency range, showing (a) the top layer, (b) the middle layer, (c) the bottom layer, and (d) the overall structure.*

The multi-functional MMA structure operating in the THz range is designed similarly to the MMA structure operating in the GHz range mentioned above. The structural parameters are presented in Table 5.2.

Parameters	p	t_d	t_m	a	R
Value (mm)	15	0.4	0.035	13.5	6
Parameters	d	l_1	l_2	l_3	l_4
Value (mm)	2.5	1.5	3	1.5	7
Parameters	l_5	l_6	l_7	w	l
Value (mm)	1.5	3	1	0.5	12

Table 5.2. Structural parameters of MMA operating in THz region

When the distance between the layers of the MMA was optimized, the absorption spectrum reached a maximum value of 98.21% at a frequency of 5.29 THz.

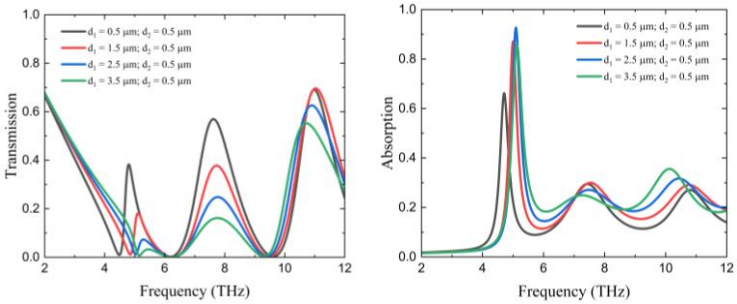

Figure 5.8. Transmission spectrum (a) and absorption spectrum (b) of the MMA structures with d_2=0.5 μm and varying d_1

5.3. Conclusion of Chapter 5

A multifunctional MMA structure operating in the GHz frequency range was designed and simulated. This multifunctional configuration comprises three distinct single-layer copper-FR4 MA structures. Following optimization, the absorption spectrum of the MMA achieves a peak value of 94.36% at 4.36 GHz.

Similarly, a multifunctional MMA operating in the THz regime was developed, consisting of three different single-layer silver-PET MA structures. After structural optimization, the absorption reaches a maximum of 98.21% at 5.29 THz.

By tuning the interlayer spacing, the interlayer interactions are modified, enabling these structures to transition between multi-band EIT and EIA. These devices achieve high transmittance at multiple frequencies in EIT mode and a peak absorption exceeding 90% in EIA mode.

Overall Conclusion

- Multi-band and broadband MMA structures operating in the GHz range, based on Cu–FR4 and graphene–FR4, were successfully designed and fabricated. The Cu–FR4 MMA achieved dual absorption peaks at 4.89 GHz and 4.97 GHz (with absorptivity >98%), while the bilayer graphene MMA exhibited an

absorption exceeding 90% across the 6.07–14.5 GHz frequency range, corresponding to a fractional bandwidth (FBW) of 81.96%.

- Multi-peak and broadband MMAs based on VO_2–Al_2O_3 were designed and simulated. When the VO_2 exhibits high conductivity (25000 S/m), corresponding to low Ohmic loss, the structure generates three intense absorption peaks at 6.68, 9.24, and 10.7 THz. Conversely, when the VO_2 has low conductivity (17500 S/m), corresponding to high Ohmic loss, the MMA transitions to a broadband absorption mode with a fractional bandwidth (FBW) of 47.89% spanning the 5.16–8.41 THz range.

- Multifunctional MMA structures operating in the GHz and THz regimes, comprising three distinct single-resonance layers, were developed. These structures exhibit the capability to switch between EIT and EIA effects. They achieve high transmittance at multiple frequencies in EIT mode and a peak absorptivity exceeding 90% in EIA mode.

The interlayer interaction mechanism in MMAs has been elucidated: high losses cause the absorption peaks to merge (approach each other), whereas low losses lead to peak separation. By employing different resonant layers and tuning the interlayer spacing, the interaction can be modulated between destructive and constructive interference. This enables the functional transition between EIT and EIA states within the metamaterial.

FUTURE RESEARCH DIRECTIONS

1. Use machine learning techniques and AI to optimize MMA structures.
2. Apply new techniques and integrate advanced materials in MMA fabrication.
3. Research and apply MMA structures for energy harvesting and gas sensing.

LIST OF PUBLICATIONS RELATED TO THE THESIS

1. Bui Xuan Khuyen, **Ngo Nhu Viet***, Pham Thanh Son, Bui Huu Nguyen, Nguyen Hai Anh, Do Thuy Chi, Nguyen Phon Hai, Bui Son Tung, Vu Dinh Lam, Haiyu Zheng, Liangyao Chen and Youngpak Lee, "Multi-layered metamaterial absorber: electromagnetic and thermal characterization", Photonics, 11, No. 3, p. 219 (2024).

2. Bui Son Tung, **Ngo Nhu Viet**, Bui Xuan Khuyen, Thanh Son Pham, Phong Xuan Do, Nguyen Thi Hoa, Vu Dinh Lam and Do Khanh Tung, "Multi-band and polarization-insensitive electromagnetically-induced transparency based on coupled-resonators in a metamaterial operating at GHz frequencies", Phys. Scr., 99 115502 (2024).

3. Thuy Chi Do, Bui Xuan Khuyen, Bui Son Tung, **Ngo Nhu Viet**, Duong Thi Ha, Vu Thi Hong Hanh, Xuan Phong Do, Do Khanh Tung∗, Hai Anh Nguyen and Vu Dinh Lam, "Wide-angle electromagnetic wave absorption via multilayer metamaterial structures", Phys. Scr., 100 025538 (2025)

4. Bui Son Tung, **Ngo Nhu Viet***, Bui Xuan Khuyen, Hai Anh Nguyen, Nguyen Khanh Viet, Phuc Vinh Nguyen, Vu Thi Van Anh and Vu Dinh Lam, "A bilayer metamaterial structure utilizing graphene ink for wide-band absorption in the GHz region", Phys. Scr., 100 085507 (2025)

5. **Ngo Nhu Viet**, Vu Dinh Lam, Bui Son Tung, Bui Xuan Khuyen, Pham Thanh Son, Nguyen Hai Anh, Nguyen Phon Hai, Do Khanh Tung, Do Thuy Chi, "Expanding the absorption bandwidth with two-layer graphene metamaterials in Gigahertz frequency range", Comm. Phys., vol. 34, no. 4, p. 365 (2024).

6. **Ngo Nhu Viet**, Bui Xuan Khuyen, Vu Dinh Lam and Bui Son Tung, "Multilayer metamaterial absorber for infrared emitter application", Proceedings of IWNA, 08-11 (2023)